Indonesian Journal of Electrical Engineering and Computer Science
Vol. 38, No. 3, June 2025, pp. 1572~1579
ISSN: 2502-4752, DOI: 10.11591/ijeecs.v38.i3.pp1572-1579

Influences from SiO_2 particles on optical properties of white diodes verified through computer simulation

Le Thi Trang[1], Nguyen Doan Quoc Anh[2]
[1]Faculty of Information Technology, Dong Nai Technology University, Bien Hoa City, Vietnam
[2]Faculty of Electrical and Electronics Engineering, Ton Duc Thang University, Ho Chi Minh City, Vietnam

Article Info

Article history:

Received Oct 28, 2023
Revised Dec 27, 2024
Accepted Feb 27, 2025

Keywords:

Light-emitting diode
$Na_3Zr_2(SiO_4)_2PO_4$: Er^{3+}/Yb^{3+}
Luminescent
Phosphors
Spectrum

ABSTRACT

For typical white-illumination diodes (WLEDs) based on phosphor conversion, heat consistency would be an essential element in phosphor samples, which is based on consistent discharge intensity, apex profile, as well as location as the samples function under different heat levels. With the goal of attaining desirable heat consistency, the study herein concerns the thermic mechanism in different phosphor samples singularly or dual-incorporated with Ce^{3+} and Eu^{2+}. Based on our acquired data, the luminescent features for the samples exhibit copious alterations when subject to different heat levels, primarily decided by phosphor bases' crystalline formation. The assessment of the interaction among the thermic mechanism and base latticework in the samples suggest that a merger between firm crystalline formations and symmetrical locations would result in desirable thermic consistency in samples. As such, the study herein also assesses a number of formations possessing firm foundations as well as specific approaches for avoiding thermic irregularities in phosphor samples, aiming to identify reliable samples as well as approaches for augmenting heat consistency for said samples.

Corresponding Author:

Nguyen Doan Quoc Anh
Faculty of Electrical and Electronics Engineering, Ton Duc Thang University
Ho Chi Minh City, Vietnam
Email: nguyendoanquocanh@tdtu.edu.vn

1. INTRODUCTION

white-illumination diodes (WLEDs) devices are well-known for desirable qualities, offering particularly vivid illumination discharge, extended durability, and greater safety. Unlike outdated lights, these devices offer greater power proficiency, being a novel illumination means for displaying purposes [1]-[3]. The common procedures for generating white illumination discharge involve employing chips based on the trio of key chromas (green, blue, red) or a merger between blue/n-UV chips and phosphor samples that constitute phosphor-transmuted Light-emitting diode (LED) devices or ptLED [4]. It is easy to construct these devices, yielding significant proficiency with less resources needed. As such, they would be employed in a large scale, becoming a ubiquitous illumination means. For generating white illumination with ptLED, it is possible to employ a merger between blue chips and YAG:Ce^{3+} or n-UV chip and trichromatic phosphor samples or blue chips and green, red phosphor samples [5]-[7]. These samples are responsible for augmenting chroma rendition indicators (CRI) as well as limiting correlated chroma temperatures (CCT) [8]. For actual uses, the mentioned chips would be employed in the form of illumination and exciting means. Said samples would be daubed above these chips, generating photo-luminescence (PL) when the chips are excited. Creating phosphor samples that yield significant proficiency as well as reliable features in proficient lights would be an essential goal [9]-[11].

Phosphor samples comprise latticework as well as triggers. While latticework barely generates illumination, they can house triggers. Typical latticework would be non-organic substances not consisting of metals include nitrides, sulfides, as well as oxides. They feature copious crystalline formations as well as adequately extensive bandgaps. Triggers would be typically deemed focal points of luminescence, generating different illumination chromas. Rare-earth as well as shift metallic elements may become triggers for having d as well f trajectories possessing copious power states that generate illumination statuses. When it comes to metallic elements, dual-valence europium as well as three-valence cerium elements are commonly employed as well as assessed for having 4f5d power levels as 4f5d shifts would be gyrate-permitted under significant quantum proficiency while 5d power states would be the furthest electronic trajectory, causing crystalline field cleavage as well as nephelauxetic outcomes decided by crystalline formations. Different illumination discharges were created via nitrides, silicates, as well as sulfides incorporated with singularly or dual-incorporated with Ce^{3+} and Eu^{2+}, while specific phosphor samples are introduced in the market for having desirable luminescent features, including YAG:Ce^{3+}, and $(Sr,Ba)_2SiO_4$:Eu^{2+}. On the other hand, the interactivity among the triggers and base latticework caused by the 5d state along with the coordinate surrounding renders the discharged illumination unreliable, especially under heat level surges that degrade sulfide, yielding toxic odor. As such, the use of phosphor samples derived from sulfide is discouraged. Heat level has an apparent effect upon phosphor samples, particularly the deterioration for the discharge intenseness (thermic abatement). Said activity may occur for various phosphor samples, lessening optical proficiency. As such, certain studies aimed to augment heat consistency in phosphor samples as well as finding novel reliable samples. Many previous works assessed the thermic mechanism in different phosphor samples, but merely addressed specific formations. As such, the findings of these works do not apply every formation. While a lot of studies addressed the thermic abatement in phosphor samples, they barely focus on the alterations for apex profile as well as location that render lights unreliable and yield lesser chroma clarity. As such, augmenting thermic consistency for phosphor samples is essential. Our primary task would be augmenting luminescent features in available phosphor samples [12]-[15].

Since the reliability in lights becomes more difficult to achieve, reliable phosphor samples prove to be a paramount factor. Beside achieving consistent discharge intenseness, it is necessary to obtain apex profile as well as phosphor location that remain the same when subject to different heat levels. As such, the study herein assesses thermic activities in different settings that feature disparate crystalline formations. The assessment concerns various aspects comprising thermic abatement, thermic deterioration, irregular thermic abatement, the extension as well as shift in discharge apexes.

2. RESEARCH METHOD

2.1. Thermic method

Typically, the discharge intenseness in phosphor samples may diminish to some extents when subject to functioning heat levels, an activity called thermic abatement. For assessing said activity, the setting coordinate graph (SCG) for Eu^{2+} as well as Ce^{3+} within the base is typically employed, exhibiting the parity location for the excited as well as ground statuses for the triggers. If the setting is simplified, the interaction between the trigger and ligands would be deemed the oscillation setting classified as parabola power form. In the case of Eu^{2+}, the electronic particles found within the ground statuses may assume excitation statuses resulting from optical excitation. Afterwards, the triggers subject to excitation may alleviate towards the parity location through incomplete power for the electronic particles being shifted towards the gyrate-latticework oscillation. Ultimately, the electronic particles subject to excitation may assume the ground status, generating illumination. Through said procedure, lattice alleviation may manifest, resulting in the trigger assuming the alleviation location. The dual latticework alleviations needed to achieve the static status would be primarily responsible for the discharge power being typically inferior to the exciting power. The disparity among the discharge and exciting power would be deemed Stokes transference, somewhat representing the firmness level in crystalline formations [16]-[18]. Thermic abatement may manifest for phosphor samples in most cases, whether the illumination discharge is generated by shift metallic elements, rare-earth metallic elements or faults, which results from thermic ionizing process as well as thermic alleviation [19].

For avoiding thermic irregularity within phosphor samples, it is necessary to manipulate the crystal formation proficiently. It is important to thoroughly assess the crystalline formation form possessing desirable thermic consistency. On the other hand, in the case of particular latticework, electron formation manipulation is advised. Typically, PL arches reliant on heat level in phosphor samples are assessed between room temperature and 250 or 300 ^{o}C. Certain studies assessed spectra under small heat level under roughly 4 K. On the other hand, only a limited number of studies concerns chilling phosphors under significant heat levels to reach room temperature. As phosphors undergo thermic processing, their discharge as well as apex location resemble unprocessed phosphors. Said inversible thermic activity would be deemed thermic

abatement. On the other hand, for certain circumstances, the phosphors' discharge intenseness would become non-reversible should they be subject to thermic processing. Liu's work concerns the luminescent features reliant on heat level for $Sr_2Si_5N_8$:0.1Eu^{2+}. The sample's discharge intenseness posterior to thermic processing suffered a 50% penalty compared to intenseness under room temperature. Said non-reversible thermic activity would be deemed thermic deterioration. In phosphor samples, thermic deterioration would be less desirable than thermic abatement. Lights' durability would be one paramount factor. Should phosphor samples exhibit limited consistency when it comes to chemicals, the lumen proficiency deteriorates overtime, resulting from the reduction for discharge intenseness posterior to multiple cycles. As such, different approaches are employed for augmenting phosphor's reliability when it comes to chemicals [20]-[22]. Thermic abatement can be absent in some phosphors. In rare cases, discharge intenseness may exhibit unusual surges under escalating heat level, an activity called irregular thermic abatement. The discharge intenseness for $LiBa_{12}(BO_3)_7F$:1%Eu^{2+} displays correlation with room temperature as the temperature rises consistently. With the surge of room temperature, the discharge intenseness surges substantially, more than threefold the starting intenseness. Afterwards, it diminishes as the phosphor undergoes further thermic processing. The phosphor yields 2 disparate TL apexes. The first apex stays under 37 ºC accompanied by significant intenseness, while the second one stays under 150 ºC accompanied by one particularly faint apex, suggesting that the phosphor comprises two forms of fixating mechanism found within the base latticework, resulting in irregular heat abatement. The thermic mechanism represents alterations for discharge intenseness as well as comprising noticeable disparities within apex profiles as well as locations. Heat level has a significant influence on latticework oscillation. If phosphors remain under significant heat levels, the potent latticework oscillation unlooses crystalline latticework. As such, it is possible for the coordinate surrounding for the triggers to shift under heat level surges. The most apparent factor would be the binding span's extension resulting from thermic extension from the base latticework. Afterwards, it is possible to alter the power for the excited statuses, matching the transposition for the discharge apex. Judging earlier works, transposition for the discharge apexes caused by thermic irregularities were found in phosphor samples such as Mg_3N_2:Eu^{2+}, and $Si_{1.92}Al_{0.08}O_{1.08}N_{1.92}$:$Eu^{2+}$.

On the other hand, the discharge apexes for these samples independently approach greater or lesser wavelengths. For assessing said apex transpositions, the luminescent features in $Ba_{2.91}Eu_{0.09}Si_6O_{15}$ (BESO) assessed in Liu's work was investigated. Unlike BESO, BESO-1200ºC as well as BESO-1300 ºC display one red-transposition at first, approaching lesser wavelengths afterwards. For identifying the transposition for discharge apexes, the SCG for Eu^{2+} under two power states within the phosphors was created. The electronic particles subject to excitation accompanying heat-functioning phonon particles may shift between the lesser power status and greater power status. Said activity would be called heat-triggered phonon-supported pathway, commonly employed for assessing the blue-transposition for discharge apexes under surging heat levels [23], [24]. The transposition for apex location would cause optical degradation for generating inconsistent discharge chromas in phosphor samples subject to functioning heat levels. As such, eliminating such an activity for illumination as well as displaying purposes would be paramount. Like discharge intenseness as well as apex location, the form for discharge apexes may alter under surging heat levels. An apparent alteration would be whole breadth under half maxima (WBHM) in discharge apexes, typically being extended. Regarding this factor, Xia's work assessed various phosphor samples such as $Ba_2Lu(BO_3)_2Cl$:0.03Eu^{2+} as well as $Ba_2Y(BO_3)_2Cl$:0.03Eu^{2+}. These samples exhibit particularly small WBHMs under room temperature. On the other hand, if heat level achieves 300 ºC, the WBHMs for the discharge apexes substantially surge. Said activity is primarily caused by the interactivity between phonon and electronic particles under significant heat levels. When it comes to illumination as well as displaying purposes, extensive WBHMs for discharge apexes generate small chroma clarity, degrading displays' performance. As such, firm crystalline formations would be paramount in phosphor samples, capable of protecting against thermic abatement, discharge apex's transposition as well as extension.

2.2. Computation method

It is possible to create a merger between electronic particles subject to excitation under the non-compact coordinate surrounding and the heat-triggered phonon particles, generating one non-radioactive shift, via Arrhenius expression [25]:

$$I_T = \frac{I_0}{1+Aexp(\frac{-\Delta E}{kT})} \quad (1)$$

I_T signifies discharge intenseness in phosphor samples under specific heat levels. I_0 signifies discharge intenseness under room temperature. ΔE signifies thermic trigger power. k signifies Boltzmann constant.

It is possible to identify the deepness of the fixating mechanism via an expression:

$$E = \frac{T_M}{500} \quad (2)$$

E signifies triggered power. T_M signifies heat level apex for TL arches. The electronic particles contained within the fixating mechanism may discharge under thermic trigger, reaching 4f5d state in Eu^{2+} that escalates the presence for the electronic particles subject to excitation. As heat levels go beyond 37 ºC, the discharge intenseness substantially exceeds the preliminary intenseness. Although said activity may yield greater lumen proficiency, the discharge chromas in the lights is altered, degrading optical performance. As such, the discharge intenseness for phosphor samples must remain consistent.

For identifying red-transpositions, it is possible to use employ Varshni expression:

$$E(T) = E_0 - \frac{aT^2}{T+b} \quad (3)$$

E(T) signifies power disparity among the ground and excited statuses under matching heat levels. E_0 signifies E(T) under 0 K. a and b signify constants related to latticework. E(T) declines as heat levels surge. On the other hand, altering the binding span invalidates the location symmetry while encouraging the Jahn-Teller activity, causing the cleavage for deteriorated excited statuses as well as diminishing E(T) that match greater wavelength discharges. As such, firm crystalline formations under minor disparities for binding spans may effectively fixating apex locations.

The interaction among WBHMs and heat levels is assessed via the expressions:

$$\mathrm{WBHM(T)} = \mathrm{W_0}\sqrt{\coth(\frac{\mathrm{hw}}{\mathrm{2kt}})} \quad (4)$$

$$W_0 = \sqrt{8ln2}(hw)\sqrt{s} \quad (5)$$

k signifies Boltzmann constant. S signifies Huang-Rhys-Pekar factor. W_0 signifies WBHM result under 0 K. hw signifies latticework oscillation power. Judging said expression, the WBHM disparity for discharge apexes primarily correlates with the latticework oscillation as well as loosen crystalline formations, extending discharge apexes under greater heat levels.

2.3. Simulation method

The experimenting process began with producing YAG:Ce^{3+}. The compound comprising preliminary substances (Y_2O_3, α-Al_2O_3, CeO_2) were made via blending the constituents within HNO_3. Afterwards, the compound underwent a firing process under 105 °C. Next, the acquired product underwent a firing process under 1,500 °C within three hours, subject to a reduction surrounding [26], [27].

SiO_2 granules featuring disparate radiuses, acquired via Aladdin Co., were blended into silicone as well as YAG:Ce^{3+}. The WLED apparatus as well as its graphical recreations is displayed Figure 1. The task of producing the LED involved the SSL formation, comprising one polycarbonate lens possessing a 12-mm diameter as well as a 6-mm height, as shown by Figures 1(a) and 1(b). An aggregate comprising nine blue chip units, an essential part in said formation shown by Figure 1(c), features one horizontal setting proportions reaching 1.14×0.1 mm, discharging illumination via one wavelength focalized at roughly 453 nm. For the goal of attaining a consistent formation, a slurry was administered unto said lens for filling the opening. Afterwards, the apparatuses underwent a curing process within one oven under 60 °C within two hours, concluding the procedure.

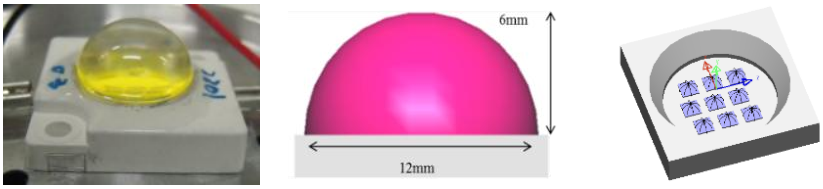

(a) (b) (c)

Figure 1. WLED setting; (a) WLED unit utilized for the study herein, (b) WLED recreated via LightTools application, and (c) recreation of multiple chips bound by wires

3. RESULTS AND DISCUSSION

Figure 2 features the changes of the scattering coefficient under different wavelengths. In Figure 2(a), the wavelength interacts with reduced scattering coefficient, while in Figure 2(b), it interacts with ordinary scattering coefficient. These changes appear to be a somewhat inverse mechanism, with the scattering coefficients slightly declining from their peaks as wavelength surges. This causes the light produced by the blue chip to spread and convert more into longer wavelength rays. As a result, the luminescence will increase when the dispersion of blue light in the forward emission rises, while the repeated absorption and back-scattering of blue light decrease. The particle size exerts its influence on CCT levels, as shown by Figure 3. The CCT is at its lowest under 2,800 K with particle size of 7 wt.%. With particle sizes of 5 wt.%, the CCT surges to the peaks under around 3,100 K.

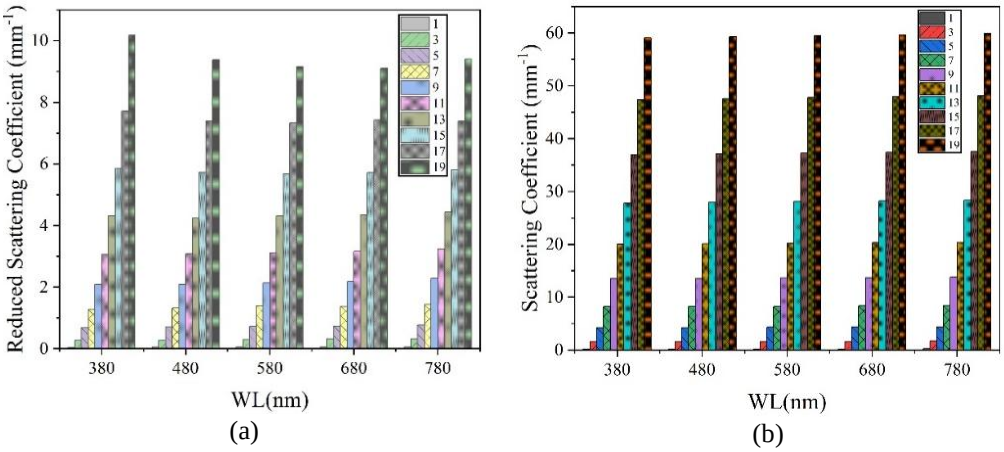

Figure 2. Relationship between reduced scattering coefficient and wavelength (a) reduced scattering coefficient and (b) scattering coefficient

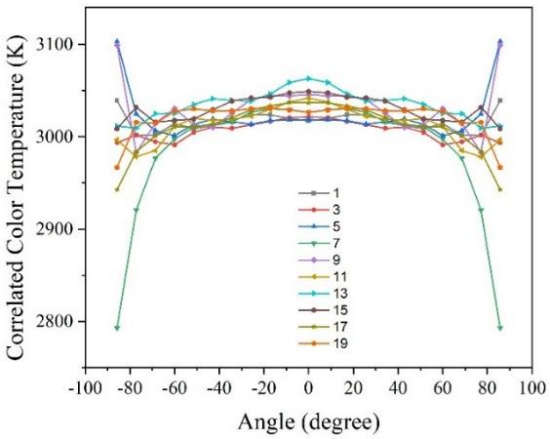

Figure 3. CCT alteration subject to particle sizes

The SiO_2 particle size has a fluctuating influence on the chroma divergence, as demonstrated via Figure 4. The chroma divergence displays considerable increases under 5, 7, and 9 µm. Notably, under 9 µm, the aberration reaches its peak, substantially surpassing all other particle sizes. For the lumen in LED shown in Figure 5, it starts out at its lowest, before undergoing a massive surge around 3 µm, then consistently surges till it reaches 9 µm. Beyond this point, the lumen exhibits various fluctuations. The observed changes might be due to differences in hue distribution and reduced blue light intensity caused by increased back-scattering and repeated absorption. Notably, with larger particle sizes, the light conversion between blue and yellow or red-orange intensifies because the phosphor layer tends to be thicker, leading to a decline in overall spectral energy. Consequently, with larger particles, the converted light may undergo back-reflection, reducing luminous intensity and resulting in a higher CCT level [28].

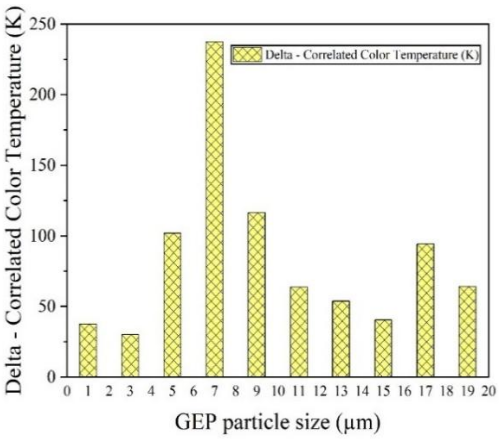

Figure 4. Chroma aberration based on particle size

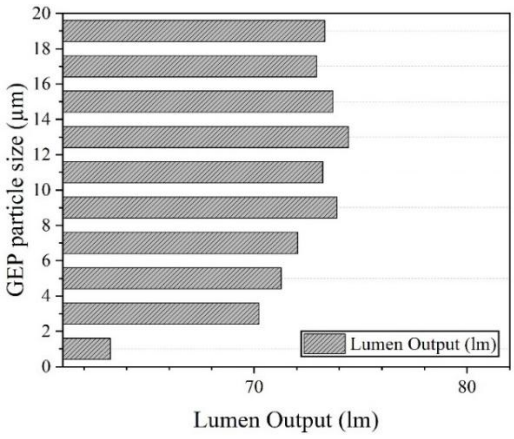

Figure 5. LED lumen under variations in SiO_2 particle size

The influence of the SiO_2 particle sizes on the chroma aberration can be seen in Figure 3. The particle size shows a fairly inconsistent effect on the chroma aberration, given the highly disparate fluctuations in the aberration. Notably, the level of chroma aberration at a particle size of 7 μm vastly surpasses those at other sizes. Other increases in chroma aberration at particle sizes of 5 μm, 9 μm as well as 17 μm are notable as well, albeit much lower than that at 7 μm. Conversely, the smallest chroma aberration is found at a particle size of 3 μm, meaning that the chroma consistency is highest at this particle size. As the SiO_2 particle size augments the scattering element, the pathway for blue illumination would be altered for greater angular levels so that the illumination may approach phosphor granules at the sheets' rim, facilitating illumination allocation around the fringes in the apparatus. Subsequently, the chroma disparity among the flank as well as direct observing angle levels would be substantially lessened, causing superior chroma consistency. As the SiO_2 particles augments scattering, the lumen output is affected as displayed via Figure 4. Under the same particle size range seen in Figure 3, the lumen shows a remarkable surge at particle sizes at 3 μm and beyond. At 9 μm and beyond, the lumen begins to show various fluctuations in a somewhat consistent trend. The peak lumen is attained at a particle size of 13 μm while the lumen at 1 μm is noticeably lower than that at any other sizes. In case the dosages for phosphor as well as SiO_2 remain the same, bigger SiO_2 particles would lessen openings among the phosphor as well as SiO_2, thus boosting the interactivity among the nanoparticles as well as blue illumination. As such, said illumination would disseminate among an extended pathway with its process of being assimilated via the phosphor showing a greater proficiency, subsequently resulting in superior intenseness for the illumination energy. Meanwhile, SiO_2 granules featuring lesser sizes boost the openings within the sheet with the blue illumination becoming fainter, yielding a lesser employment proficiency for blue illumination through phosphors. As the particle sizes reach a particular point, the lumen begins to fluctuate. This is caused by a greater presence of blue illumination assimilated by substrates, resulting from rear reflection. Ultimately, different particle sizes can yield different advantages and disadvantages. While a lower particle size can yield the most desirable consistency in chroma, larger counterparts can offer a better lumen output. It depends on the manufacturing criteria on optical qualities to come up with the most appropriate particle size.

4. CONCLUSION

The study herein concerns the thermic mechanism for specific phosphor samples. As heat levels surge, thermic abatement would be the clearest degradation for luminescent features in phosphor samples. With the goal of remedying said downside, various approaches including regulating coordinate surrounding for triggers, dual incorporation for triggers, daubing phosphors as well as fault utilization. Judging the alteration for apex profiles as well as location under surging heat level, firm as well as symmetric crystal formations prove to be a paramount factor. With the purpose of attaining particularly symmetrical locations, it is possible to employ superseding approach as well as hard compound for regulating coordinate surrounding for triggers. Firm as well as symmetrical three-dimension formations can guarantee desirable thermic consistency in phosphor samples. With the criteria concerning proficient lights as well as displaying devices becoming more demanding, it is possible to configure reliable phosphor samples for constructing more desirable WLED devices.

FUNDING INFORMATION

Authors state no funding involved.

AUTHOR CONTRIBUTIONS STATEMENT

Name of Author	C	M	So	Va	Fo	I	R	D	O	E	Vi	Su	P	Fu
Le Thi Trang		✓	✓	✓	✓	✓			✓	✓				
Nguyen Doan Quoc Anh	✓	✓	✓	✓	✓	✓	✓	✓	✓	✓	✓	✓	✓	

C : **C**onceptualization
M : **M**ethodology
So : **So**ftware
Va : **Va**lidation
Fo : **Fo**rmal analysis
I : **I**nvestigation
R : **R**esources
D : **D**ata Curation
O : Writing - **O**riginal Draft
E : Writing - Review & **E**diting
Vi : **Vi**sualization
Su : **Su**pervision
P : **P**roject administration
Fu : **Fu**nding acquisition

CONFLICT OF INTEREST STATEMENT

Authors state no conflict of interest.

DATA AVAILABILITY

The data that supports the findings of this study are openly available in International Journal of Technology at https://doi.org/10.14716/ijtech.v15i1.6165, reference number [25]; in Materials Science-Poland at https://doi.org/10.2478/msp-2020-0002, reference number [26]; in IJECE at http://doi.org/10.11591/ijece.v10i4.pp4015-4022, reference number [27]; in TELKOMNIKA at http://doi.org/10.12928/telkomnika.v18i4.13723, reference number [28]

REFERENCES

[1] P. T. Tin, N. K. H. Nguyen, M. Q. H. Tran, and H.-Y. Lee, "Red-emitting α-SrO·3B_2O_3:Sm^{2+} Phosphor for WLED Lamps: novel lighting properties with two-layer remote Phosphor package," *Current Optics and Photonics*, vol. 1, no. 4, pp. 389–395, Aug. 2017, doi: 10.3807/copp.2017.1.4.389.

[2] J. Li, Z. Li, G. Liang, S. Yu, Y. Tang, and X. Ding, "Color uniformity enhancement for COB WLEDs using a remote phosphor film with two freeform surfaces," *Optics Express*, vol. 24, no. 21, p. 23685, 2016, doi: 10.1364/oe.24.023685.

[3] L.-Y. Chen *et al.*, "Novel broadband glass phosphors for high CRI WLEDs," *Optics Express*, vol. 22, no. S3, p. A671, 2014, doi: 10.1364/oe.22.00a671.

[4] T. Yang, B. Glorieux, K. Shiau, Y. Chang, Y. Yu, and C. Sun, "Improving light output by micro-TiO_2 scatters in pc-WLED encapsulants," *Optics Express*, vol. 30, pp. 47082-47092, 2022, doi: 10.1364/OE.476096.

[5] J. Hao, H. L. Ke, L. Jing, Q. Sun, and R.T. Sun, "Prediction of lifetime by lumen degradation and color shift for LED lamps, in a non-accelerated reliability test over 20,000 h," *Applied Optics*, vol. 58, pp.1855-1861, 2019, doi: 10.1364/AO.58.001855.

[6] A. K. Dubey, M. Gupta, V. Kumar, and D. S. Mehta, "Laser-line-driven phosphor-converted extended white light source with uniform illumination," *Applied Optics*, vol. 58, pp.2402-2407, 2019, doi: 10.1364/AO.58.002402.

[7] S. An, J. Zhang, and L. Zhao, "Optical thermometry based on upconversion luminescence of Yb^{3+}-Er^{3+} and Yb^{3+}-Ho^{3+} doped Y6WO12 phosphors," *Applied Optics*, vol. 58, pp.7451-7457, 2019, doi: 10.1364/AO.58.007451.

[8] T. DeLawyer, M. Tayon, C. Yu, and S. L. Buck, "Contrast-dependent red-green balance shifts depend on S-cone activity," *Journal of the Optical Society of America*, vol. 35, pp.B114-B121, 2018, doi: 10.1364/JOSAA.35.00B114.

[9] W. Gao, K. Ding, G. He, and P. Zhong, "Color temperature tunable phosphor-coated white LEDs with excellent photometric and colorimetric performances," *Applied Optics*, vol. 57, pp. 9322-9327, 2018, doi: 10.1364/AO.57.009322.

[10] D. T. Tuyet *et al.*, "Deep red fluoride dots-in-nanoparticles for high color quality micro white light-emitting diodes," *Optics Express*, vol. 28, pp. 26189-26199, 2020, doi: 10.1364/OE.400848.

[11] J. X. Yang, D. S. Li, G. Li, E. Y. B. Pun, and H. Lin, "Photon quantification in Ho3+/Yb3+ co-doped opto-thermal sensitive fluotellurite glass phosphor," *Applied Optics, vol. 59*, pp. 5752-5763, 2020, doi: 10.1364/AO.396393.

[12] D. Yan, S. Zhao, H. Wang, and Z. Zang, "Ultrapure and highly efficient green light emitting devices based on ligand-modified CsPbBr3 quantum dots," *Photonics Research*, vol. 8, pp. 1086-1092, 2020, doi: 10.1364/PRJ.391703.

[13] L. Xie, *et al.*, "Highly luminescent and stable lead-free cesium copper halide perovskite powders for UV-pumped phosphor-converted light-emitting diodes," *Photonics Research*, vol. 8, pp. 768-775, 2020, doi: 10.1364/PRJ.387707.

[14] L. Li, Y. Zhou, F. Qin, Y. Zheng, and Z. Zhang, "On the Er3+ NIR photoluminescence at 800 nm," *Optics Express*, vol. 28, pp. 3995-4000, 2020, doi: 10.1364/OE.386792.

[15] H. E. A. Mohamed, K. Hkiri, M. Khenfouch, S. Dhlamini, M. Henini, and M. Maaza, "Optical properties of biosynthesized nanoscaled Eu2O3 for red luminescence applications," *Journal of the Optical Society of America*, vol. 37, pp. C73-C79, 2020, doi: 10.1364/JOSAA.396244.

[16] Y. Peng, X. Guo, R. Li, H. Cheng, and M. Chen, "Thermally stable WLEDs with excellent luminous properties by screen-printing a patterned phosphor glass layer on a microstructured glass plate," *Applied Optics*, vol. 56, pp. 3270-3276, 2017, doi: 10.1364/AO.56.003270.

[17] J. Zhou and K. Qian, "Low-voltage wide-field-of-view lidar scanning system based on a MEMS mirror," *Applied Optics*, vol. 58, pp. A283-A290, 2019, doi: 10.1364/AO.58.00A283.
[18] J. Li, Y. Tang, Z. Li, X. Ding, L. Rao, and B. Yu, "Investigation of stability and optical performance of quantum-dot-based LEDs with methyl-terminated-PDMS-based liquid-type packaging structure," *Optics Letters*, vol. 44, pp. 90-93, 2019, doi: 10.1364/OL.44.000090.
[19] T. Y. Orudzhev, S. G. Abdullaeva, and R. B. Dzhabbarov, "Increasing the extraction efficiency of a light-emitting diode using a pyramid-like phosphor layer," *Journal of Optical Technology*, vol. 86, pp. 671-676, 2019, doi: 10.1364/JOT.86.000671.
[20] Y. Chang, *et al.*, "An advanced laser headlight module employing highly reliable glass phosphor," *Optics Express*, vol. 27, pp. 1808-1815, 2019, doi: 10.1364/OE.27.001808.
[21] L. Zan, D. Lin, P. Zhong, and G. He, "Optimal spectra of white LED integrated with quantum dots for mesopic vision," *Optics Express*, vol. 24, no. 7, p. 7643, Mar. 2016, doi: 10.1364/oe.24.007643.
[22] X. Li, S. Zhou, R. Wei, X. Liu, B. Cao, and H. Guo, "Blue–green color-tunable emissions in novel transparent Sr_2LuF_7:Eu/Tb glass-ceramics for WLEDs," *Chinese Optics Letters*, vol. 18, no. 5, p. 051601, 2020, doi: 10.1364/COL.18.051601
[23] Z. Zhao *et al.*, "Site selective and enhanced blue emitting of Eu^{2+} activated fluorapatite-type phosphors with high color purity for NUV excited pc-wLEDs," *Optical Materials Express*, vol. 12, no. 10, pp. 4117-4132, 2022, doi: 10.1364/OME.470850.
[24] Y. Peng *et al.*, "Flexible fabrication of a patterned red phosphor layer on a YAG:Ce^{3+} phosphor-in-glass for high-power WLEDs," *Optical Materials Express*, vol. 8, no. 3, p. 605, 2018, doi: 10.1364/ome.8.000605.
[25] K.-J. Chen *et al.*, "Enhanced luminous efficiency of WLEDs using a dual-layer structure of the remote phosphor package," *Journal of Lightwave Technology*, vol. 31, no. 12, pp. 1941-1945, 2013, doi: 10.1109/JLT.2013.2260322
[26] M.-J. Chen *et al.*, "The impacts of Ba2Li2Si2O7:Sn2+, Mn2+ and CaMgSi2O6:Eu2+,Mn2+ particles on the optical properties of remote phosphor LED," *Materials Science-Poland*, vol. 38, no. 1, pp. 197–205, Mar. 2020, doi: 10.2478/msp-2020-0002.
[27] J. Cheng *et al.*, "Photoluminescence properties of $Ca_4La_6(SiO_4)_4(PO_4)_2O_2$-based phosphors for wLEDs," *Chinese Optics Letters*, vol. 17, no. 5, p. 051602, 2019, doi: 10.3788/col201917.051602.
[28] M. Guan, Y. Wu, Z. Kuang, S. Xu, and J. Zhang, "Efficient and tunable emission $CsPbClxBr_3$–x quantum dot glass for overcoming the lack of cyan gap in WLED," *Optics Letters*, vol. 48, no. 19, p. 5173, 2023, doi: 10.1364/ol.503970.

BIOGRAPHIES OF AUTHORS

Le Thi Trang received a Master's degree in Information Technology from Lac Hong University, Vietnam, and is currently working as a lecturer at the Faculty of Information Technology, Dong Nai Technology University, Bien Hoa City, Vietnam. Her research interests include computer science, computer vision, image recognition and classification, face detection and recognition, abnormal motion detection, and graphic design. She can be contacted at email: lethitrang@dntu.edu.vn.

Nguyen Doan Quoc Anh was born in Khanh Hoa province, Vietnam. He has been working at the Faculty of Electrical and Electronics Engineering, Ton Duc Thang University. Quoc Anh received his Ph.D. degree from National Kaohsiung University of Science and Technology, Taiwan in 2014. His research interest is optoelectronics. He can be contacted at email: nguyendoanquocanh@tdtu.edu.vn.